Acta Neuropathol (2014) 127:523–538
DOI 10.1007/s00401-013-1220-8

ORIGINAL PAPER

Early loss of oligodendrocytes in human and experimental neuromyelitis optica lesions

Claudia Wrzos · Anne Winkler · Imke Metz · Dieter M. Kayser · Dietmar R. Thal · Christiane Wegner · Wolfgang Brück · Stefan Nessler · Jeffrey L. Bennett · Christine Stadelmann

Received: 8 July 2013 / Revised: 7 November 2013 / Accepted: 20 November 2013 / Published online: 30 November 2013

Abstract Neuromyelitis optica (NMO) is a chronic, mostly relapsing inflammatory demyelinating disease of the CNS characterized by serum anti-aquaporin 4 (AQP4) antibodies in the majority of patients. Anti-AQP4 antibodies derived from NMO patients target and deplete astrocytes in experimental models when co-injected with complement. However, the time course and mechanisms of oligodendrocyte loss and demyelination and the fate of oligodendrocyte precursor cells (OPC) have not been examined in detail. Also, no studies regarding astrocyte repopulation of experimental NMO lesions have been reported. We utilized two rat models using either systemic transfer or focal intracerebral injection of recombinant human anti-AQP4 antibodies to generate NMO-like lesions. Time-course experiments were performed to examine oligodendroglial and astroglial damage and repair. In addition, oligodendrocyte pathology was studied in early human NMO lesions. Apart from early complement-mediated astrocyte destruction, we observed a prominent, very early loss of oligodendrocytes and oligodendrocyte precursor cells (OPCs) as well as a delayed loss of myelin. Astrocyte repopulation of focal NMO lesions was already substantial after 1 week. Olig2-positive OPCs reappeared before NogoA-positive, mature oligodendrocytes. Thus, using two experimental models that closely mimic the human disease, our study demonstrates that oligodendrocyte and OPC loss is an extremely early feature in the formation of human and experimental NMO lesions and leads to subsequent, delayed demyelination, highlighting an important difference in the pathogenesis of MS and NMO.

Keywords Neuromyelitis optica · Demyelination · Oligodendrocyte death · Experimental autoimmune encephalomyelitis · Astrocyte

Electronic supplementary material The online version of this article (doi:10.1007/s00401-013-1220-8) contains supplementary material, which is available to authorized users.

C. Wrzos · A. Winkler · I. Metz · C. Wegner · W. Brück · S. Nessler · C. Stadelmann (✉)
Institute of Neuropathology, University Medical Centre Göttingen, Robert-Koch-Str. 40, 37099 Göttingen, Germany
e-mail: cstadelmann@med.uni-goettingen.de

D. M. Kayser
Institute of Pathology, Städtisches Klinikum Görlitz, Görlitz, Germany

D. R. Thal
Institute of Pathology/Laboratory for Neuropathology, University of Ulm, Ulm, Germany

J. L. Bennett
Departments of Neurology and Ophthalmology, University of Denver, Colorado, USA

Introduction

Neuromyelitis optica (NMO) is a chronic inflammatory demyelinating disease that has long been considered a variant of multiple sclerosis (MS). Recently, antibodies against aquaporin-4 (AQP4) have been identified as a specific disease marker of NMO [12, 13]. Pathologically, NMO is characterized by destructive demyelinating lesions, i.e., lesions which are typically devoid of astrocytes as well as myelin, and which show substantial axonal loss [16, 17, 23]. The most characteristic feature of NMO, however, is the destruction of astrocytes and their foot processes in early lesions, substantiating the cardinal role of astrocyte pathology in disease. Additional histological features that distinguish NMO from MS include perivascular

immunoglobulin (Ig) and complement deposition, vascular hyalinosis and the presence of polymorphonuclear—and especially eosinophilic—granulocytes in the early inflammatory infiltrate [16, 23, 32].

Anti-AQP4 antibodies are found in the sera of around 75 % of NMO patients, depending on the sensitivity of the assay applied [6, 12, 13, 40, 41]. Their titres have been shown to correlate loosely with disease severity and length of spinal cord involvement [9, 22, 37]. Intravenous transfer of recombinant monoclonal anti-AQP4 antibodies derived from a CSF plasma cell of an NMO patient induced astrocyte loss in an animal model of perivenous CNS inflammation [1]. Similarly, the transfer of sera derived from NMO patients led to perivascular astrocyte loss in experimental autoimmune encephalomyelitis (EAE)-based rodent models [3, 11], demonstrating the pathogenicity of anti-AQP4 antibodies in vivo. AQP4 is a water channel expressed at particularly high density on astrocytic endfeet abutting the capillaries in specialized 3-dimensional structures, so-called orthogonal arrays [5, 28, 43]. High antigen densities are found in the optic nerves and spinal grey matter [32]. Besides mediating astrocyte loss, anti-AQP4 antibodies may downregulate AQP4 and excitatory amino acid transporter (EAAT)2 on astrocytic endfeet with ensuing astrocyte dysfunction [7].

NMO lesions closely resemble MS lesions, especially with regard to demyelination and the presence of foamy macrophages and lymphocytic inflammation. However, in contrast to the majority of MS lesions, abundant apoptotic oligodendrocytes have been reported in and immediately adjacent to early NMO lesions [4, 26]. Given that astrocytes are considered the primary target in NMO, the time course and mechanisms of oligodendroglial and myelin damage are of particular interest. In addition, NMO lesions with different degrees of astroglial repopulation have been described. Bipolar, presumably recently generated astrocytes are frequently found in early NMO lesions [26]. However, the time course and sequence of astrocytic repair, oligodendroglial repopulation, and remyelination have yet to be examined.

In the present study, we employed two experimental models to examine the time course of myelin and oligodendroglial damage as well as oligodendroglial and astroglial repopulation in NMO-like lesions: (1) a transfer model of recombinant human anti-AQP4 antibodies (NMO rAb) into MBP (myelin-basic protein)-primed rats ("NMO/EAE") [1]; and (2) a "focal NMO" model involving the focal, intracerebral stereotactic injection of NMO rAb and human complement. The NMO/EAE and focal NMO models provide complementary data on NMO CNS injury in the presence and absence of a CNS-specific T-cell response and allow investigation of the temporal course of glial injury and recovery in experimental NMO lesions.

Materials and methods

Human NMO tissue

CNS tissue from six patients with serologically confirmed NMO or NMO spectrum disease was included in our study (Table 1). 4/6 patients had undergone brain or spinal cord biopsy for diagnostic purposes to exclude tumor, lymphoma or infection. From two patients, we analyzed CNS tissue obtained at autopsy. Anti-AQP4 disease was neuropathologically confirmed by a focal loss of GFAP and AQP4 in macrophage-rich, inflammatory demyelinating lesions with relative axonal preservation. In addition to the diagnostic histological and immunohistochemical stainings applied, tissue sections were stained for NogoA and Olig2. The study was approved by the local ethics committee.

Animals

All experiments were carried out in adult (170–240 g) female inbred Lewis rats ($n = 139$) purchased from Harlan Winkelmann GmbH (Borchen, Germany). The animals were kept in cages of 6 animals each on a 12:12 h light/dark cycle with food and water ad libitum. All experiments

Table 1 Clinical characteristics of patients with anti-AQP4-seropositive NMO or NMO spectrum disease who were included in the study

Patient no.	B/A	Age/sex	Disease duration (years)	Disease course	CNS involvement	Lesions studied
1	B	37/w	9	RR	Brain, spinal cord, optic nerve	Occipital brain lesion
2	B	31/w	5	RR	Brain, spinal cord, optic nerve	Parietal brain lesion
3	B	57/m	10	RR	Brain, spinal cord	Parietal brain lesion
4	B	45/w	2	RR	Spinal cord	Spinal lesion
5	A	77/w	24	RR	Brain, spinal cord, optic nerve	Spinal lesion
6	A	72/m	0.75	RR	Brain, spinal cord	Periventricular brain lesion

All patients were seropositive for anti-AQP4 antibodies and harbored early lesions at biopsy or autopsy

A autopsy, *B* biopsy, *f* female, *m* male, *RR* relapsing-remitting

were accredited by the Bezirksregierung Braunschweig, Germany.

Intravenous injection of NMO rAbs in MBP-preimmunized rats (EAE/NMO model)

The recombinant human anti-AQP4 antibody 53 (NMO rAb), derived from a CSF plasma cell of an NMO patient [1] (500 µl; $c = 5$ mg/ml; $n = 8$), or a control human rAb 2B4 (ctrl rAb) against measles virus nucleocapsid protein (500 µl; $c = 5$ mg/ml; $n = 4$), respectively, was transferred into the retrobulbar venous plexus of female Lewis rats previously immunized with guinea pig (gp)$MBP_{72–85}$-peptide emulsified in complete Freund's adjuvant containing 2.5 mg/ml inactivated *Mycobacterium tuberculosis* H37 Ra. Alternatively, variants of NMO rAbs containing point mutations reducing complement-dependent cytotoxicity (CDC) [NMO rAb_no CDC (K322A), $n = 2$] or antibody-dependent cell-mediated cytotoxicity (ADCC) (NMO rAb_no ADCC [K326W/E333S], $n = 2$) were i.v. injected [31, 38, 44]. The rAbs were applied 7–9 days after immunization at a clinical disease score of 1.0–1.5 (tail paralysis and/or mild righting abnormalities). Rats with EAE were scored according to Weissert et al. [42]. The rats were euthanized 30 h after i.v. rAb injection, and brains and spinal cords were dissected and processed for paraffin embedding.

Induction of focal astrocyte depletion in the rat brain by intracerebral stereotactic injection of NMO rAbs (focal NMO model)

Rats were anesthetized i.p. by ketamine/xylazine and mounted in a stereotactic frame. A rostro-caudal cut was performed to give access to the skull. A small hole was drilled into the skull 1 mm caudal and 2 mm lateral to the bregma to uncover the surface of the brain. A finely calibrated glass capillary (Ø = 0.05–0.1 mm) was then stereotactically inserted, targeting the motor cortex or underlying corpus callosum (1.7–2.2 mm depth), respectively. The rats were then injected with a total volume of 1 µl of NMO rAb, NMO rAb_no ADCC ($n = 8$) or NMO rAb_no CDC ($n = 8$) ($c = 2.5$ mg/ml) diluted in NMO-IgG negative human serum or PBS with purified human complement (Sigma-Aldrich) over a 3-min period. Control animals were injected with human serum or complement alone, heat-inactivated serum together with NMO rAb or human serum or complement together with ctrl rAb. Monastral blue (Sigma-Aldrich) was added as a marker dye to trace the injection site. After injection, the glass capillary was carefully withdrawn and the operation site was sealed by suture. The animals were perfused at various time points after injection (1 h, 3 h, 24 h, 3 days, 1 week, 2 weeks, 4 weeks), and the brains were dissected and processed for paraffin embedding.

Histology and immunohistochemistry

Brain and spinal cord tissue was sectioned and evaluated for inflammation, myelin disruption and astrocyte destruction by hematoxylin/eosin and Luxol fast blue (LFB)/periodic acid-Schiff (PAS) staining and immunohistochemistry for AQP4 (AQP4; Millipore, Billerica, MA), glial fibrillary acidic protein (GFAP; Dako, Glostrup, Denmark), S100β (Abcam, Cambridge, UK), excitatory amino acid transporter 2 (EAAT2, GLT-1; Novocastra, Newcastle, UK), myelin-basic protein (MBP; Dako, and SMI 94, Covance, Princeton, NJ, USA), myelin-associated glycoprotein (MAG, kindly provided by C. Richter-Landsberg, Oldenburg, and T.V. Waehneldt, Göttingen [19]), rat anti-myelin oligodendrocyte glycoprotein (MOG) antiserum, SMI 91 [2′,3′-cyclic-nucleotide 3′-phosphodiesterase (CNP; Covance)] and proteolipid protein (PLP; Biozol, Eching, Germany). Additionally, antibodies against rat C9 (kindly provided by B.P. Morgan, Cardiff, UK), human IgG (BioGenex, The Hague, Netherlands), CD3 (Serotec, Düsseldorf, Germany), Iba-1 (Wako, Neuss, Germany) and CD68 (ED1, Serotec) were used to detect complement, human IgG, $CD3^+$ T cells, microglia and macrophages/activated microglia, respectively. Axon pathology was shown by Bielschowsky silver impregnation and immunohistochemistry for amyloid precursor protein (APP; Chemicon, Temecula, CA) as described previously [20]. To assess mature oligodendrocytes and oligodendrocyte precursor cells, NogoA (mAb 11C7 [25], kindly provided by M.E. Schwab, Brain Research Institute, Department of Neuromorphology, University and ETH Zurich) and Olig2 (IBL, Hamburg, Germany) immunohistochemistry were performed. Biotinylated secondary antibodies followed by avidin-peroxidase and diaminobenzidine were used to visualize antibody binding. Polymorphonuclear cells were visualized by detecting chloroacetate esterase by enzyme histochemistry (Naphthol AS-D Chloroacetate esterase kit; Sigma-Aldrich, Steinheim, Germany).

Quantification of NogoA- and Olig2-positive oligodendroglial cells

Cell densities were evaluated at a 400× magnification using an ocular morphometric grid. In the EAE/NMO model Olig2- and NogoA-positive cells were counted in astrocyte-depleted lesions of 5 spinal cord cross sections per animal after NMO rAb injection, whereas random grey and white matter areas were assessed in ctrl rAb-injected animals (NMO rAb-injected rats: $n = 8$; ctrl rAb-injected rats: $n = 4$). Means of lesion and normal-appearing grey and white matter cell densities were calculated for each rat. In focal NMO (each group: $n = 5$) Olig2- and NogoA-positive cells were counted in one brain lesion per animal; in

animals injected with ctrl rAb cells were evaluated near the injection site. In the human brain and spinal cord, NogoA- and Olig2-positive cells were counted in areas of astrocyte loss as well as in the periplaque white matter (PPWM).

Quantification of the loss of astrocytic proteins (GFAP, AQP4, EAAT2, S100β)

The extent of astrocyte loss in experimental NMO lesions was assessed using GFAP immunohistochemistry (IHC). In addition, the loss of AQP4, EAAT2 and S100β was quantified after focal NMO lesion induction. Immunostained spinal cord or brain sections were scanned using a BX51 Olympus light microscope equipped with a DP71 digital camera. Areas of complete loss of immunoreactivity were measured using AnalySIS (Soft imaging System®, Münster, Germany). 10–15 spinal cord cross sections were examined per animal in the EAE/NMO model (NMO rAb-injected rats: $n = 8$; ctrl rAb-injected rats: $n = 4$). Data are given as percentage of GFAP-free area per whole measured spinal cord area. Loss of immunoreactivity of GFAP, AQP4, EAAT2 and S100β was quantified in five animals per group with stereotactically induced focal NMO lesions. Graphs indicate mean cell numbers per animal whereby each data point corresponds to one animal.

Statistical analysis

Data were analyzed and graphs generated using GraphPad Prism Version 5 for Windows (GraphPad Software, San Diego, CA, USA). For statistical comparison of two or more experimental groups, unpaired *t* test or one-way ANOVA was applied. If variances were significantly different, Welch's correction was used. Non-parametric tests (Mann–Whitney or Kruskal–Wallis, followed by Dunn's post-test) were performed if the data did not follow a Gaussian distribution. Data are presented as mean ± SD. A p value ≤ 0.05 was considered significant.

Results

Intravenous transfer of human NMO rAbs leads to perivascular astrocyte depletion and a more severe disease course in rat EAE

Human NMO lesions contain perivascular and parenchymal CD4- and CD8-positive T cells [16, 32, 39]. However, to date, only mild perivascular infiltrates without astrocytic loss have been generated by direct immunization of experimental animals with AQP4 protein or AQP4 peptides [24, 27]. To enhance the penetration of NMO antibodies into the CNS parenchyma, NMO rAbs were injected intravenously into Lewis rats preimmunized with guinea pig $MBP_{72\text{-}85}$ peptide. MBP immunization on its own has been reported to only lead to perivascular T cell and macrophage infiltration, but no relevant demyelination or astrocyte loss [1, 14, 15, 45]. Transfer of NMO rAb, but not ctrl Ab, into MBP-immunized rats produced large perivenous astrocyte-depleted areas, predominantly in the spinal cord, where the majority of perivascular inflammatory infiltrates were localized (Fig. 1a–m; Mann–Whitney test; $p = 0.0095$). Importantly, significantly higher mean maximum EAE scores were attained by animals transferred with NMO rAb (Mann–Whitney test; $p = 0.0377$; Fig. 1n). On serial sections, spinal lesions showed a similar size on IHC for AQP4, GFAP, S100β and EAAT2 (Fig. 1a–d). Suppl. Fig. 1 highlights the predominantly perivenous lesion distribution with loss of astrocytes or astrocytic proteins only in animals injected with NMO rAb (Suppl. Fig. 1i–l), but not in controls injected with ctrl rAb (Suppl. Fig. 1a–d). These findings support the notion that NMO rAbs predominantly lead to a depletion of astrocytes in the grey (GM) and white matter (WM) in the EAE/NMO model, but not to a substantial downregulation of AQP4 protein in the lesion penumbra (Fig. 1a–d; Suppl. Fig. 1i–l).

Both experimental groups—injected either with ctrl (Suppl. Fig. f) or NMO rAb (Fig. 1j; Suppl. Fig. 1n)—showed similar T cell infiltration induced by immunization with MBP-peptide (Suppl. Fig. 1f). Increased numbers of foamy macrophages were observed in astrocyte-depleted areas (Fig. 1k; Suppl. Fig. 1o) compared to controls (Suppl. Fig. 1g). Perivascular C9 (Fig. 1e) and human IgG deposits (Fig. 1f) were detected after NMO rAb injection. In addition, a marked infiltration by polymorphonuclear granulocytes was observed 30 h after NMO rAb transfer (Fig. 1g). At this time point, these animals showed initial signs of acute axon damage detected by APP staining, whereby the amount exceeded the axonal injury observed after MBP immunization alone (Fig. 1h). Axonal loss was not evident by Bielschowsky silver impregnation at this time point (Fig. 1i; Suppl. Fig. 1p). Additionally, astrocyte-depleted areas showed mild perivascular demyelination and myelin vacuolization (Fig. 1l; Suppl. Fig. 1m), which was not seen in ctrl rAb-injected rats (Suppl. Fig. 1e).

Astrocyte depletion is complement-dependent

To exclude potential confounding effects caused by non-AQP4-specific lymphocytic inflammation due to prior immunization, we developed a focal NMO model similar to that previously described in mice [35]. Circumscribed astrocyte-depleted lesions were observed after stereotactic injection of small volumes (1 µl) of human NMO rAb together with human serum or complement into the rat cortex or white matter, respectively (Fig. 2a, d). In contrast,

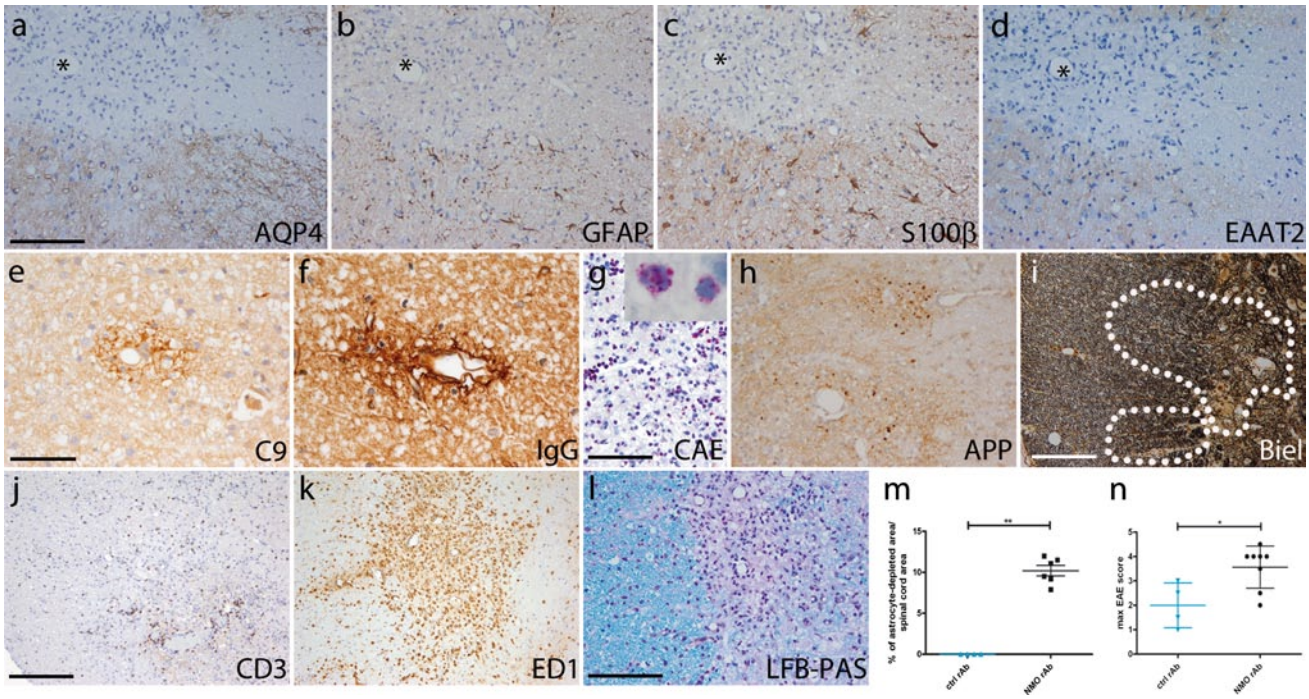

Fig. 1 Astrocyte depletion by NMO rAb in spinal lesions in EAE rats. Loss of astrocytic proteins (**a** AQP4, **b** GFAP, **c** S100β, **d** EAAT2) is present 30 h after antibody transfer in the EAE/NMO model. *Asterisks* indicate the same vessel on serial sections. Perivascular complement (**e** C9) and human IgG (**f** human IgG) depositions in NMO/EAE. Perivascular lesions are also infiltrated by polymorphonuclear cells [**g** chloroacetate esterase (CAE), *inset* shows enlarged polymorphonuclear cells], T cells (**j** CD3) and macrophages/activated microglia (**k** ED1). Mild perivascular demyelination is seen in GFAP-depleted areas (**l** LFB/PAS). APP-positive axonal spheroids are present within astrocyte-depleted lesions (**h**); however, axons are well preserved (**i** Bielschowsky silver impregnation). The astrocyte-depleted area is significantly larger in NMO rAb compared to ctrl rAb-injected rats with EAE (**m** $^{**}p = 0.0095$, Mann–Whitney test). Of note, the mean maximum clinical scores are higher in NMO rAb-injected rats (**n** $^{*}p = 0.0377$, Mann–Whitney test; NMO rAb: $n = 8$; ctrl rAb: $n = 4$). The *dotted line* delineates the astrocyte-depleted area. *Blue* ctrl rAb, *black* NMO rAb. *Scale bars* 100 μm (**a**–**d**, **g**, **h**, **l**), 50 μm (**e**, **f**), 200 μm (**i**–**k**)

injection of human recombinant-anti measles antibody (2B4) (ctrl rAb) alone or diluted in serum (data not shown), heat-inactivated human serum with NMO rAb (Fig. 2b, e) or human serum alone (Fig. 2c, f) did not induce astrocyte loss or loss of AQP4 expression. Similar results were obtained using purified human complement preparations (data not shown).

These findings were confirmed by the focal intracerebral injection of a mutant recombinant human anti-AQP4-antibody lacking the complement-binding site (NMO rAb_no CDC), which produced significantly smaller astrocyte-depleted lesions compared to "wild-type" NMO rAb injection. Similarly, the use of a mutant antibody with reduced ability to activate ADCC (NMO rAb_no ADCC), led to significantly diminished lesion size (NMO rAb: 1.1 ± 0.5 mm^2; NMO rAb_no CDC: 0.4 ± 0.3 mm2; NMO rAb_no ADCC: 0.15 ± 0.3 mm^2; one-way ANOVA; $^{**}p < 0.001$; $^{***}p < 0.0001$; Fig. 2g). Assessing the contribution of antibody effector functions in the systemic NMO/EAE model, we found that astrocyte loss was nearly prevented by injecting the mutant antibody lacking CDC function (GFAP-depleted area in % of total spinal cord cross-sectional area: NMO rAb: 13 ± 7 % vs. NMO rAb_no CDC: 1.3 ± 0.9 %; Fig. 2h). In addition, we observed less GFAP loss after applying the antibody mutant deficient in ADCC (NMO rAb_no ADCC: 6 ± 2 %; Fig. 2h). This indicates that CDC as well as ADCC contributes to NMO lesion formation in both our models.

Rapid loss of oligodendrocytes after astrocyte depletion

NMO is generally considered a demyelinating disease, however, it remains unclear how this humoral immune reaction against astrocytes exactly leads to demyelination. Taking advantage of the EAE/NMO model, NogoA- and Olig2-positive oligodendroglial cells were analyzed in astrocyte-depleted lesions 30 h after NMO rAb transfer. Quantification of NogoA-positive cells in sections co-stained for GFAP (purple) and NogoA (brown) revealed a significant ~48 % decrease of mature oligodendrocytes in EAE/NMO lesions [NMO rAb-transferred rats ($n = 8$);

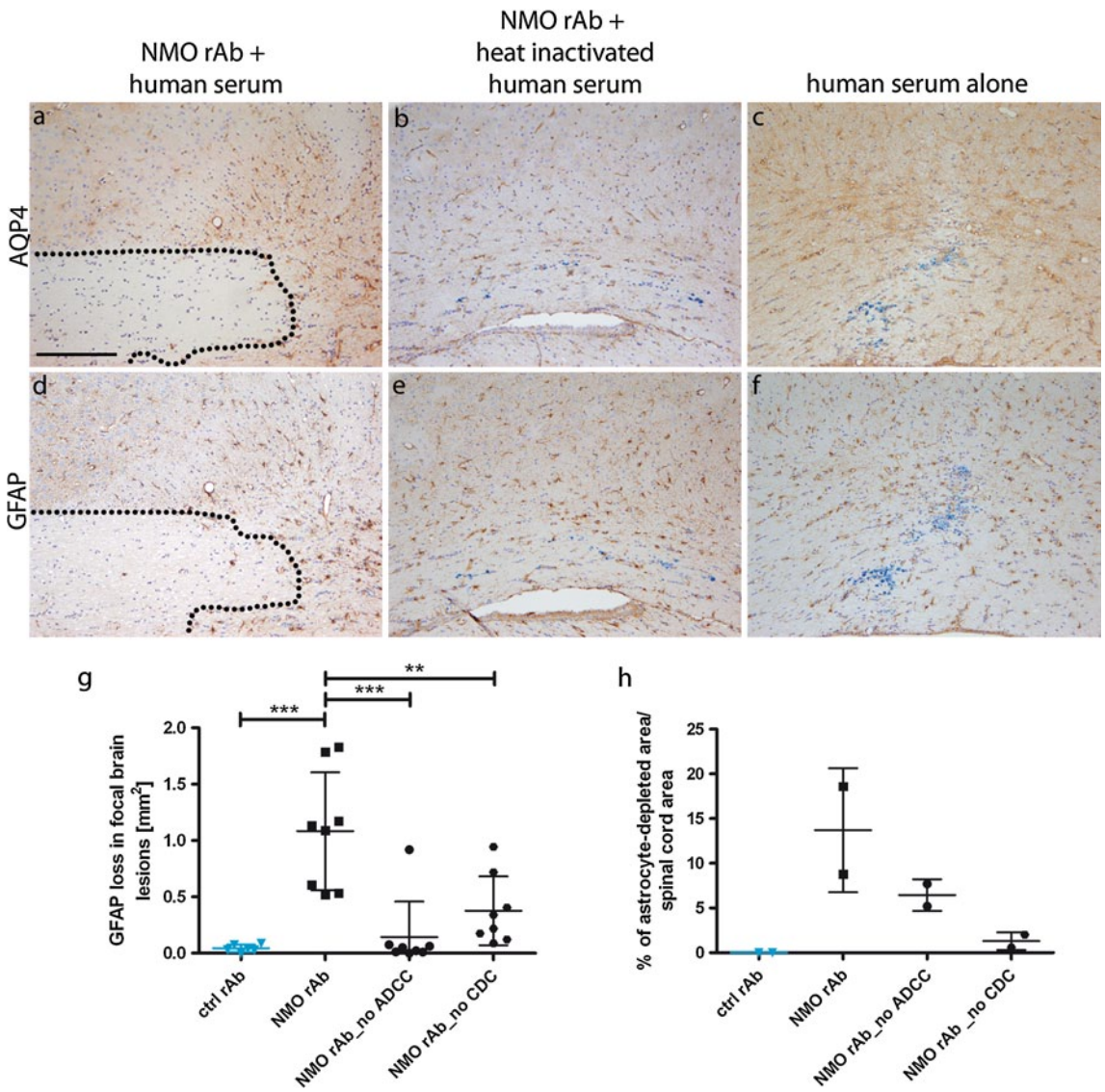

Fig. 2 Astrocyte depletion is complement-dependent in both the focal NMO and EAE/NMO model. Injection of NMO rAb diluted in human serum induces a prominent astrocyte-depleted lesional area in the brain as visualized by anti-AQP4 (**a**) and anti-GFAP (**d**) immunohistochemistry (IHC). Injection of NMO rAb together with heat-inactivated serum did not induce significant astrocyte loss (**b** AQP4, **e** GFAP). Similarly, no astrocyte loss was seen when animals were injected with human serum alone (**c** AQP4, **f** GFAP). A significant reduction of the GFAP-depleted lesion areas in the brain was observed when animals were focally injected with mutant recombinant antibodies lacking efficient complement activation (NMO rAb_no CDC; $^{**}p < 0.001$, one-way ANOVA; **g**) or ADCC (NMO rAb_no ADCC; $^{***}p < 0.0001$, one-way ANOVA; NMO rAb: $n = 8$; ctrl rAb: $n = 8$; NMO rAb_no ADCC: $n = 8$; NMO rAb_no CDC: $n = 8$; **g**). Also, i.v. injection of these point-mutated antibodies reduced the size of spinal astrocyte-depleted lesions in the EAE/NMO model compared to "wild-type" NMO rAb (NMO rAb: $n = 2$; ctrl rAb: $n = 2$; NMO rAb_no ADCC: $n = 2$; NMO rAb_no CDC: $n = 2$; **h**). *Monastral blue marks* the injection site (**a**–**f**). The *dotted line* indicates the astrocyte-depleted area. *Scale bar* 200 μm

117 ± 22 cells/mm^2; Fig. 3a, e] compared to animals transferred with ctrl rAb ($n = 4$; 224 ± 12 immunopositive cells/mm^2; $p < 0.0001$, t test; Fig. 3b, e). Similarly, a significant loss of ~52 % of Olig2-positive OPCs (brown) was observed in NMO rAb-transferred rats compared to controls (NMO rAb: 71 ± 28 cells/mm^2 (Fig. 3c, f); ctrl rAb: 148 ± 31 cells/mm^2 (Fig. 3d, f); $p = 0.004$, Mann–Whitney test).

To delineate the time course of oligodendroglial loss, early stages of NMO lesion development were studied in the focal NMO model. Already 1 h after lesion initiation, a reduction of astrocyte density and retraction of astrocytic processes were seen (Fig. 4a, b). However, NogoA- and Olig2-positive oligodendroglial cells still remained well preserved, as were the myelin sheaths at this early time point (Fig. 4c–e). 3 h after focal NMO

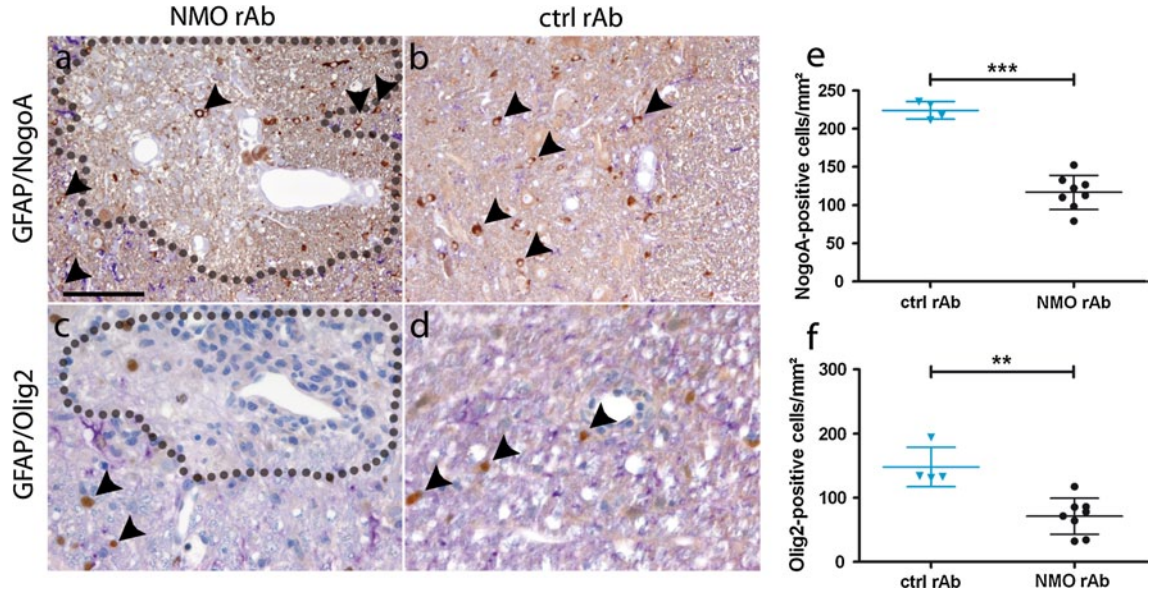

Fig. 3 Extensive loss of oligodendroglial cells in the EAE/NMO model. Double stainings for GFAP (*purple*) and NogoA (*brown*) depict the reduction of NogoA-positive cells in spinal lesions from NMO rAb (**a**) but not ctrl rAb (**b**) injected animals. Double stainings for GFAP (*purple*) and Olig2 (*brown*) picture the demise of Olig2-positive cells in EAE rats injected with NMO rAb (**c**) but not with ctrl rAb (**d**). A significant reduction of mature NogoA-positive oligodendrocytes is found in the spinal cord of EAE rats injected with NMO rAb ($n = 8$) compared to ctrl rAb ($n = 4$; $p < 0.0001$, t test; **e**). Similarly, the density of Olig2-positive oligodendroglia is significantly reduced in NMO rAb-injected animals ($p = 0.004$, Mann–Whitney test; **f**). *Dotted lines* indicate the astrocyte-depleted area. *Blue* ctrl rAb, *black* NMO rAb. *Scale bar* 100 μm

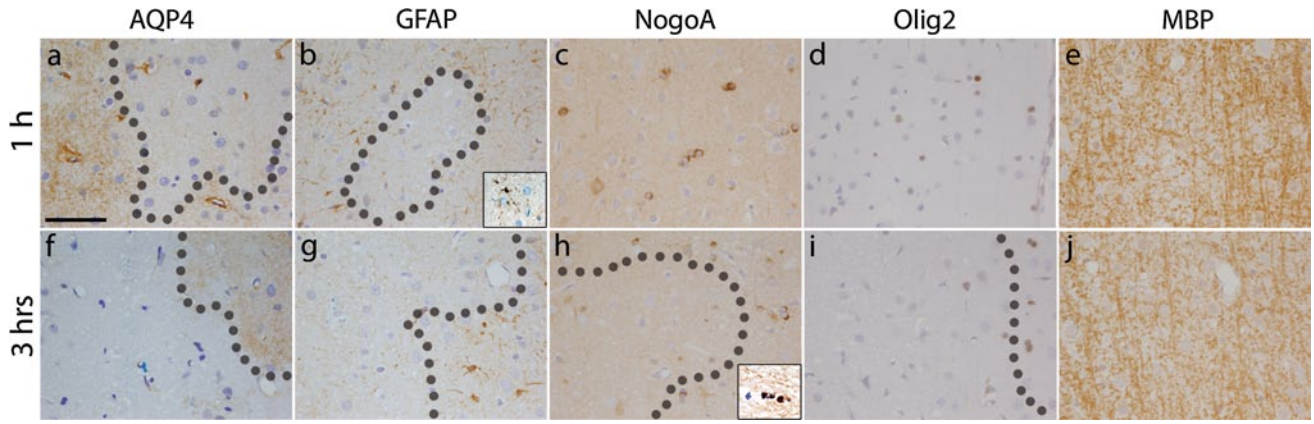

Fig. 4 Oligodendroglial loss occurs early in focal NMO lesions. Already 1 h after intracerebral NMO rAb injection (**a**–**e**), there is a reduction in astrocyte density [**a** AQP4, **b** GFAP (*inset* damaged astrocyte)]. At this time point, no oligodendroglial loss or demyelination is visible (**c** NogoA, **d** Olig2, **e** MBP). 3 h after lesion induction (**f**–**j**), astrocyte loss is already substantial (**f** AQP4, **g** GFAP). Additionally, loss of mature oligodendrocytes [**h** NogoA (*inset* damaged oligodendrocyte)] and OPCs is prominent (**i** Olig2), but loss of myelin is not yet apparent (**j** MBP). The *dotted line* delineates the astrocyte-depleted area. *Monastral blue marks* the injection site (**a**–**j**). *Scale bar* 50 μm

rAb injection, the astrocyte-depleted area was already well demarcated on GFAP- and AQP4-immunostained sections (Fig. 4f, g). At this time point, a reduction of oligodendroglial cells was already apparent (Fig. 4h, i); however, the myelin sheaths still appeared intact (Fig. 4j).

Oligodendrocyte and oligodendrocyte precursor loss are features of early human NMO lesions

We examined oligodendrocyte densities in astrocyte-depleted lesions in cerebral and spinal biopsies and autopsies from anti-AQP4-seropositive patients (Table 1). Early

NMO lesions were characterized by a focal loss of LFB-positive myelin sheaths (Fig. 5a), relative axonal preservation (Fig. 5b), infiltration of KiM1P-positive foamy macrophages that largely also expressed the early antigen MRP14 (Fig. 5c, d) and reduction of GFAP- and AQP4-immunoreactivity (Fig. 5e, f). Scattered T cells were observed perivascularly as well as in the parenchyma (Fig. 5g, h). A few polymorphonuclear cells were also detected (Fig. 5i). Furthermore, deposition of IgG (Fig. 5j) and activated complement components (C9neo) was found (Fig. 5k). Oligodendroglial cells as identified by CNP (l), NogoA (m), or Olig2 (*n*) immunohistochemistry were markedly reduced in early NMO lesions. The densities of NogoA- and Olig2-positive oligodendroglia were quantified in areas of GFAP- and/or AQP4-loss as well as in the periplaque white matter (PPWM) (NMO lesions: $n = 6$ patients; PPWM: $n = 5$ patients). NogoA-positive mature oligodendrocytes were present at a density of 274 ± 59 cells/mm^2 in the PPWM (set to 100 %) and significantly reduced to 4.9 % (14 ± 13 cells/mm^2) in lesions ($p = 0.0006$, *t* test with Welch correction; Fig. 5o). Similarly, Olig2-positive oligodendroglia were significantly decreased to 1.3 % in lesions (5 ± 3 cells/mm^2) compared to PPWM (266 ± 125 cells/mm^2 set to 100 %); ($p = 0.0096$, *t* test with Welch correction; Fig. 5p).

Infiltration of polymorphonuclear granulocytes and macrophages occurs after oligodendroglial demise

We hypothesized that inflammatory mediators released by polymorphonuclear granulocytes or invading macrophages might contribute to oligodendroglial cell death. We thus performed time-course experiments assessing inflammatory cell infiltration 1 h, 3 h, 24 h and 1 week after induction of astrocyte depletion in the focal NMO model. Surprisingly, no invading ED1-positive macrophages/activated microglia (Fig. 6a, b) or polymorphonuclear granulocytes (PMNs) (Fig. 6i, j), but only few microglia (Fig. 6e, f) were detected 1 or 3 h after focal astrocyte depletion, when oligodendroglial cell death was already apparent (Fig. 9). However, at 24 h, substantial infiltration by macrophages/activated microglia and granulocytes was observed (Fig. 6c, g, k). Dense infiltration by macrophages/activated microglia with only a few remaining granulocytes was found 1 week after focal astrocyte depletion (Fig. 6d, h, l). The density of ED1-positive cells gradually decreased until week 4, the latest time point examined (Fig. 9).

Rapid astrocyte repopulation already 1 week after lesion initiation

Little is known about astrocyte repair of human NMO lesions. Bipolar astrocytes, most likely representing regenerating astroglia, have been described in early human NMO lesions (Fig. 5e) [4, 26]. Using AQP4, GFAP, S100β and EAAT2 as astrocytic markers, we assessed the time frame of astrocytic repopulation and reoccurrence of marker protein expression in focal NMO lesions (Figs. 7a–q, 9). 24 h after induction of focal NMO, astrocyte-depleted areas lacked AQP4, GFAP, S100β and EAAT2 immunoreactivity to a similar extent (Fig. 7a–d, q). One week after lesion initiation, astrocytes had already repopulated ~86 % of the formerly depleted lesion area (Fig. 7e–h, q; GFAP-depleted area after 24 h: 0.72 ± 0.3 mm^2; after 1 week: 0.09 ± 0.04 mm^2; $p < 0.0001$, Kruskal–Wallis with Dunn's multiple comparison test). However, expression of EAAT2 was still significantly decreased at this time point ($p < 0.05$, Kruskal–Wallis with Dunn's multiple comparison test; Fig. 7d, h, q). 2 weeks after lesion initiation the lesion area was already fully repopulated, showing an upregulation of AQP4 and GFAP, reflecting astrogliosis (Fig. 7i, j, m, *n*). However, expression of S100β and EAAT2 was not yet completely back to normal levels (Fig. 7k, l, o, p, q).

OPC recruitment is paralleled by astrocyte repopulation and precedes the appearance of NogoA-positive mature oligodendrocytes

We hypothesized that oligodendroglial repopulation and maturation within focal NMO lesions might be slow given the near-total destruction of precursor cells and lack of astrocytes. 24 h after focal NMO lesion induction, a substantial reduction of NogoA-positive cells by ~77 % and of Olig2-positive cells by ~83 % of was observed in astrocyte-depleted areas compared to ctrl rAb-injected animals (Figs. 8a, b, q, r, 9). Myelin appeared pale on MBP IHC (Fig. 8c; Suppl. Fig. 2). One week after lesion induction, NogoA-positive cells were still reduced by ~70 %, whereas

Fig. 5 Significant reduction of NogoA and Olig2-positive oligodendroglia in early human NMO lesions. A representative NMO lesion (patient 4) is depicted showing loss of myelin (**a** LFB/PAS), axonal distension, but preservation (**b** Bielschowsky silver impregnation), infiltration by KiM1P (**c**)—and in part MRP14-positive macrophages (**d**), reduction of GFAP-positive astrocytes (**e**), loss of AQP4-immunoreactivity (**f**), scattered infiltration by CD3 (**g**)—and CD8 (**h**)-positive T cells, some polymorphonuclear granulocytes (**i**, Giemsa), IgG (**j**, patient 6) and activated complement [**k** C9neo (*red*)] depositions. Importantly, oligodendroglial cells are largely lost within the demyelinated and astrocyte-depleted lesion evidenced by CNP (**l**), NogoA (**m**) and Olig2 immunohistochemistry (**n**). Quantification of NogoA- and Olig2-positive cells in astrocyte-depleted lesions and the periplaque white matter (PPWM) of patients with NMO or NMO spectrum disease revealed a significant loss of oligodendroglia in lesions compared to PPWM (**o**, **p** *t* test with Welch correction, $^{**}p = 0.0096$, $^{***}p = 0.0006$; NMO lesions: $n = 6$ patients; PPWM: $n = 5$ patients). *Arrows* indicate IHC-positive cells. **a**, **d** Original magnification ×40, *scale bar* 500 μm; **b**, **c**, **e**, **f**, **l** *scale bar* 200 μm; **g**, **h**, **j**, **k**, **m**, **n** *scale bar* 50 μm; **i** *scale bar* 20 μm

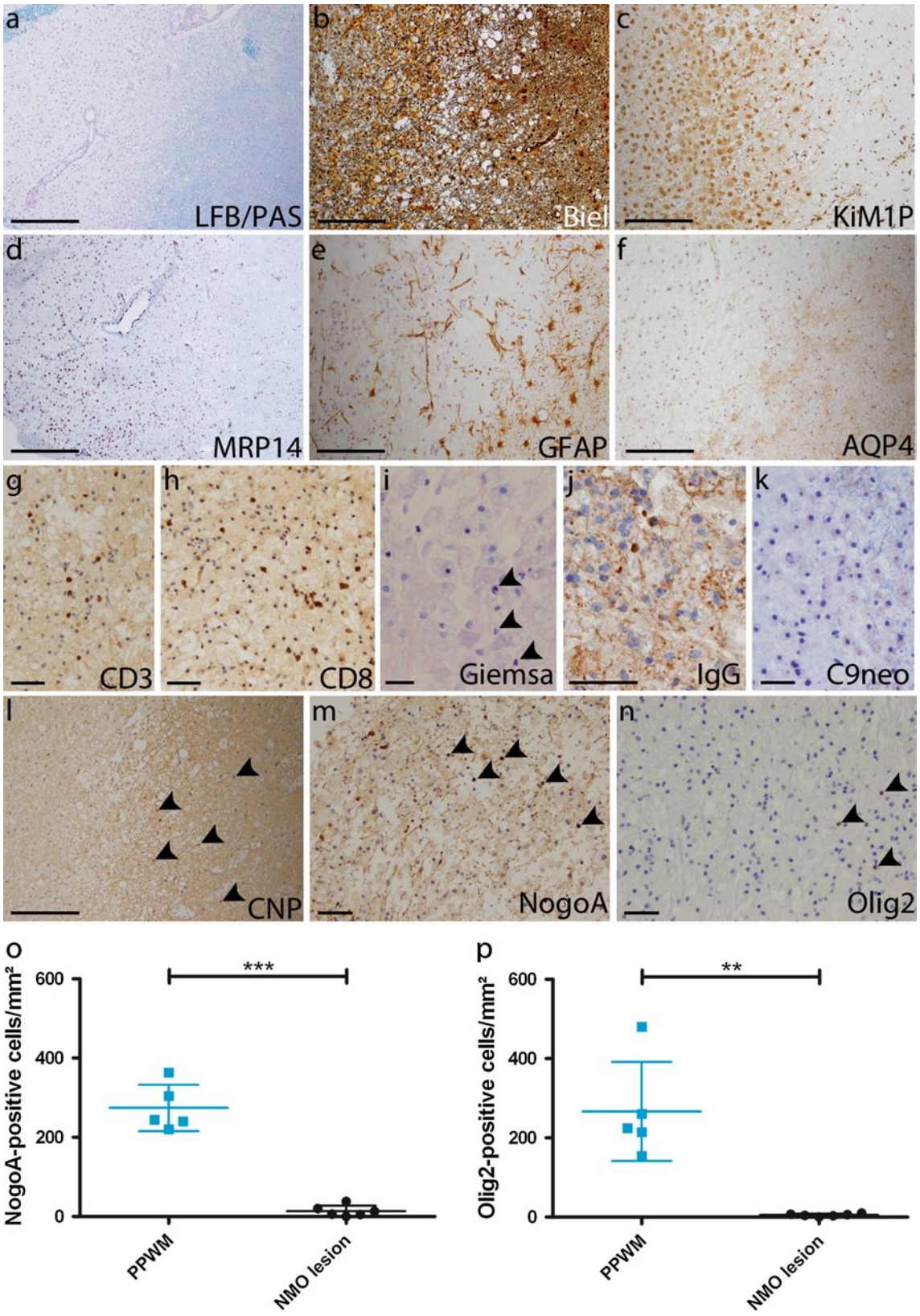

Olig2-positive cells were abundant throughout the lesion area (Fig. 8e, f, q, r). At this time point, a fully demyelinated area with fuzzy borders was apparent (Fig. 8g; Suppl. Fig. 2). 2 and 4 weeks after lesion induction, abundant NogoA- (Fig. 8i, m, q) and Olig2-positive cells (Fig. 8j, n, r) were found in the lesions. Remyelination was nearly

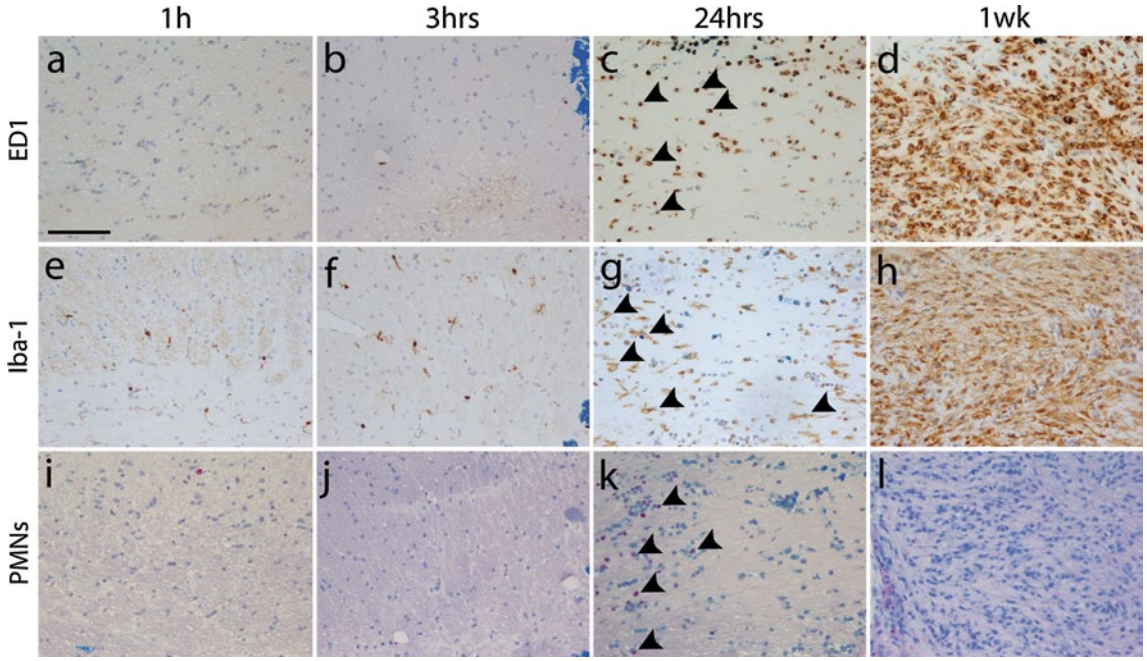

Fig. 6 Polymorphonuclear granulocytes and macrophages/activated microglia infiltrate after oligodendroglial demise in the focal NMO model. No infiltration by ED1-positive macrophages/activated microglia 1 h (**a**) and 3 h (**b**) after induction of focal NMO. Only single Iba-1-positive ramified microglia are detected (**e**, **f**). After 24 h ED1- (**c**) and Iba-1-positive (**g**) cell numbers increase reaching their highest densities after 1 week (**d**, **h**). 1 h (**i**) and 3 h (**j**) after lesion induction no polymorphonuclear granulocytes (PMNs) are detected. At 24 h (**k**), many PMNs are present but have disappeared 1 week later (**l**) (**i**–**l** chloroacetate esterase, *pink*). *Arrows* indicate stained cells. *Monastral blue marks* injection site. *Scale bar* 100 μm

complete at week 4 (Fig. 8o). Axons were relatively preserved throughout lesion formation and resolution (Fig. 8d, h, l, p).

The quantification of NogoA-positive cells in focal lesions confirmed the complete repopulation of lesions with NogoA-positive oligodendrocytes at week 2 (after 24 h, 53 ± 16 cells/mm^2; after 1 week, 70 ± 28 cells/mm^2; after 2 weeks, 229 ± 37 cells/mm^2; ctrl rAb after 24 h, 231 ± 58 cells/mm^2; $p < 0.0001$, one-way ANOVA) (Figs. 8q, 9). In contrast, repopulation by Olig2-positive cells already occurred 1 week after lesion induction (after 24 h, 39 ± 13 cells/mm^2; after 1 week, 221 ± 49 cells/mm^2; ctrl rAb after 24 h, 189 ± 42 cells/mm^2; $p < 0.0001$, one-way ANOVA) (Figs. 8r, 9).

Discussion

NMO is an inflammatory demyelinating disease of the CNS with substantial similarities to MS, both clinically and pathologically. In NMO astrocytes have been identified as the targets of a destructive humoral immune response. The links between astrocyte damage and demyelination, however, remain unclear. Using two different experimental models based on recombinant human anti-AQP4 antibodies and early human NMO biopsy tissue, we report here that oligodendroglial death rapidly follows astrocytic demise leading to secondary demyelination. We furthermore confirm, using a mutant recombinant antibody, that complement-mediated astrocyte depletion is a crucial process in lesion initiation. In addition, ADCC contributes to astrocyte destruction in our models. With regard to lesion repair, we show that astrocyte repopulation in the focal NMO model takes approximately 1 week. On the contrary, only few mature NogoA-positive oligodendrocytes are detectable at that time point. This study thus underlines fundamental differences in the mechanisms of demyelination between MS and NMO.

In a first set of antibody transfer experiments, we took advantage of an established monophasic rat EAE model, namely immunization of Lewis rats with gpMBP-peptide. This model leads to perivenous mononuclear infiltration 7–10 days after immunization predominantly in the spinal cord, with ascending paralysis followed by recovery within several days [42]. We injected NMO rAb at the onset of clinical symptoms, thus allowing the antibody access to the CNS [1]. Animals injected with NMO rAbs showed a more severe EAE disease score [3], and the lesions generated closely resembled human NMO lesions with perivenous astrocyte depletion, perivascular complement and Ig

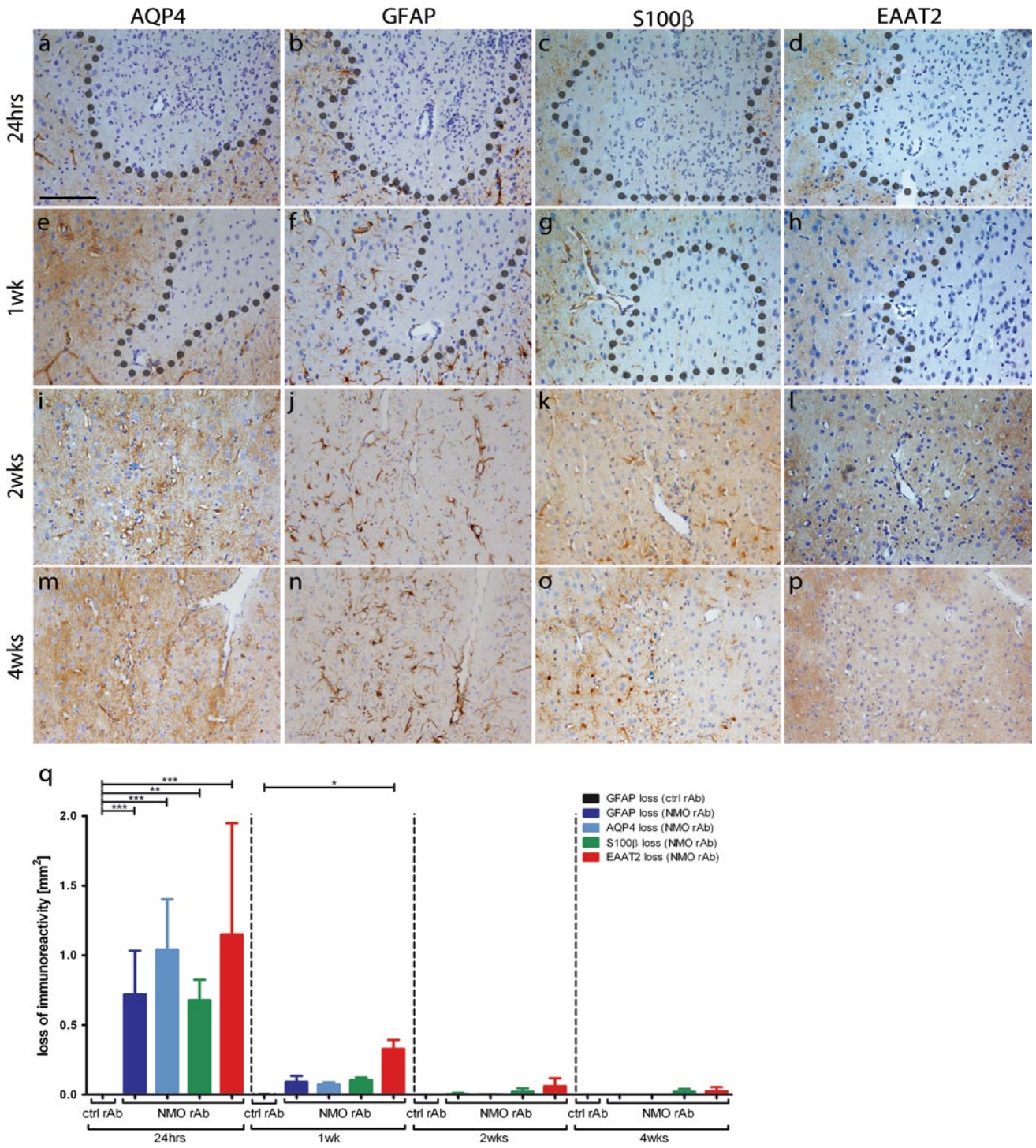

Fig. 7 Rapid repopulation of focal NMO lesions by astrocytes. 24 h after intracerebral NMO rAb injection, a prominent loss of astrocytes (**a** AQP4, **b** GFAP, **c** S100β, **d** EAAT2, **q** $p < 0.0001$, Kruskal–Wallis with Dunn's multiple comparison test) is observed. Already 1 week after lesion induction, astrocyte repopulation is substantial (**e** AQP4, **f** GFAP, **g** S100β, **h** EAAT2, **q**). After 2 weeks, astrocyte repopulation appears nearly complete (**i** AQP4, **j** GFAP, **k** S100β, **l** EAAT2, **q**). 4 weeks after lesion induction the area of former astrocyte depletion is fully repopulated and shows an upregulation of AQP4 (**m**) and GFAP (**n**), whereas the expression of S100β (**o**) and EAAT2 (**p**) is still slightly reduced. For each time point and condition $n = 5$ animals per group are included in the analysis. *Monastral blue marks* the injection site. *Scale bar* 100 μm

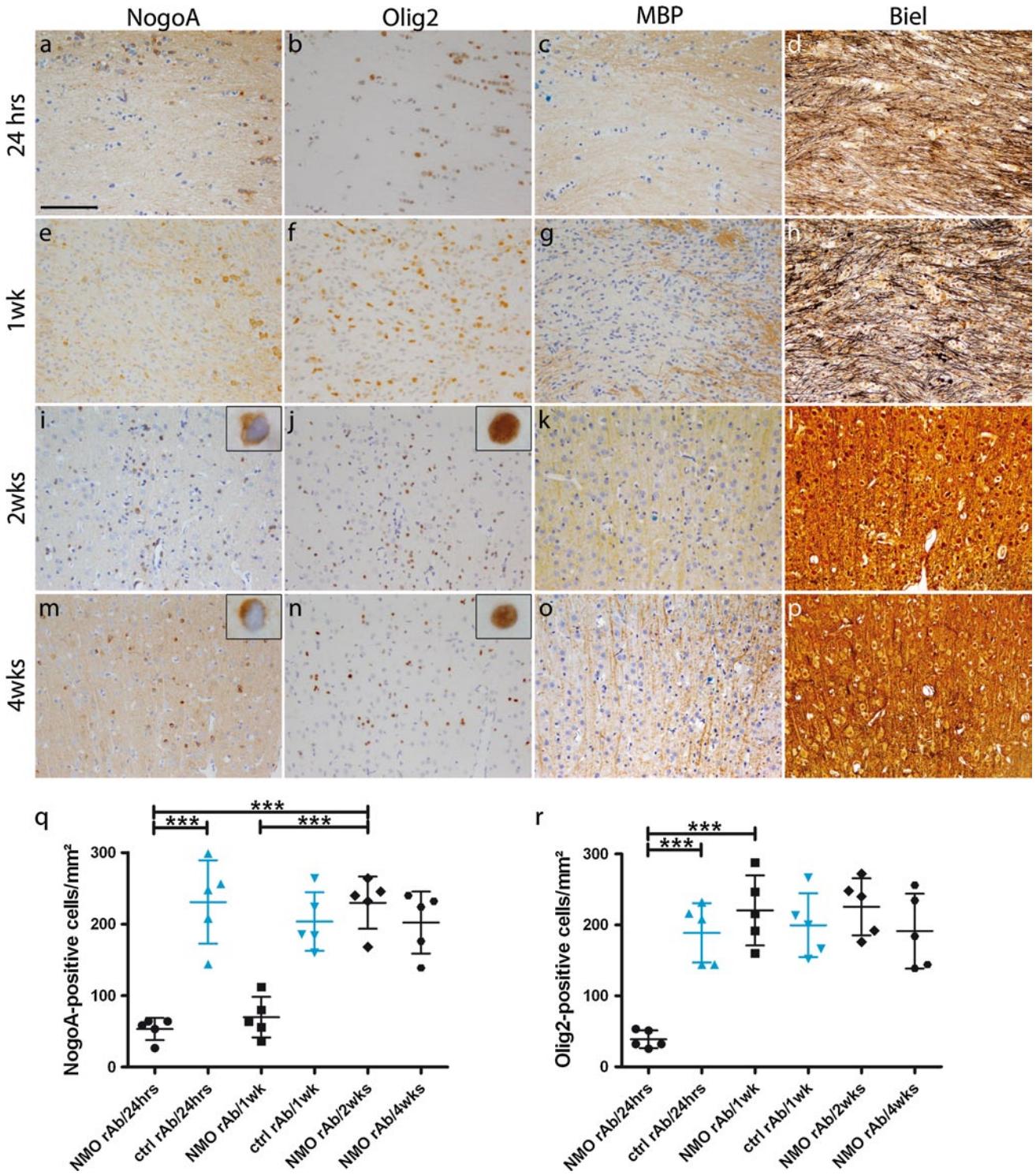

deposition, and infiltration by T cells, neutrophilic granulocytes and macrophages, with predominantly spinal lesion localization. 30 h after antibody injection, myelin appeared pale and in part vacuolized, but no fully demyelinated lesions were observed. In contrast, oligodendroglial cells were already markedly reduced, and there was substantial acute axonal damage [1, 3, 11].

Interestingly, the complete features of human NMO have yet to be reproduced by immunization with AQP4 peptides or protein alone [10, 24, 27]. The transfer of AQP4-peptide-specific T cell lines in rats resulted in mononuclear inflammatory infiltration in the CNS parenchyma, and the additional transfer of AQP4-specific antibodies produced mild perivenous and subpial astrocyte loss [27].

◀ **Fig. 8** Repopulation by NogoA-positive cells follows rapid Olig2 recruitment in focal NMO lesions. Animals injected with NMO rAb reveal a significant loss of NogoA-positive (**a** NogoA, **q** one-way ANOVA, $p < 0.0001$) and Olig2-positive (**b** Olig2, **r** one-way ANOVA, $p < 0.0001$) cells/mm^2 24 h after focal NMO lesion induction, not seen in ctrl rAb-injected animals (**q**). At that time point myelin pallor (**c** MBP), in the presence of morphologically well preserved axons (**d** Bielschowsky silver impregnation), is observed. One week after intracerebral injection numbers of NogoA-positive cells are still decreased (**e** NogoA, **q**), whereas Olig2-positive cells have returned to normal levels (**f** Olig2, **r** one-way ANOVA, $p < 0.0001$) and remain stable at weeks 2 (**j**, **r**) and 4 (**n**, **r**). MBP IHC reveals a demyelinated area with fuzzy borders (**g**) and preserved axons (**h** Bielschowsky silver impregnation) after 1 week. After 2 weeks numbers of mature oligodendrocytes have returned to near normal densities (**i** NogoA, **q** one-way ANOVA, $p < 0.0001$) and are stable at week 4 (**m**, **q**). This is paralleled by remyelination (**k**, **o** MBP) and morphologically intact axons (**l**, **p** Bielschowsky silver impregnation) at weeks 2 and 4. Injection of the ctrl rAb with human complement did not significantly influence oligodendroglial cell counts at any time point (**q**, **r**). For each time point and condition $n = 5$ animals per group are included in the analysis. *Monastral blue marks* the injection site. *Blue* ctrl rAb, *black* NMO rAb. *Scale bar* 100 μm

The combined results suggest that particular features of cellular and humoral immunity may be necessary to produce pathognomonic NMO histopathology. Therefore, the EAE/NMO model facilitates the study of NMO lesion formation, development and repair by providing a highly predictable disease course and substantial perivenous spinal cord inflammation and astrocyte depletion. However, it should be noted that MBP-specific T cells have so far not been found to play a role in the human disease.

To further study the extent and time course of tissue damage elicited by NMO rAbs alone, without perivenous T-lymphocytic inflammation, we applied a focal stereotactic NMO model based on intracerebral injection of human NMO rAbs. We used patch clamp capillaries (Ø = 0.05–0.1 mm) for stereotactic injection to minimize traumatic tissue injury [21]. Furthermore, a minimal fluid volume of 1 μl was injected over a 3-min period. Hence, we could confirm that astrocyte depletion by NMO rAbs is rapid and dependent on complement activation [35]. A mutant antibody with reduced CDC function produced no or only minimal astrocyte injury in either model system. Activated complement components are a hallmark of early NMO lesions, and in addition may link astrocyte injury with subsequent oligodendrocyte destruction [23, 32]. The current data therefore provide further support for blocking antibody effector function in the treatment of acute NMO exacerbations [29, 38, 44].

Interestingly, a mutant antibody with diminished ADCC effector function [31, 38, 44] also showed reduced astrocyte depletion in our NMO/EAE antibody transfer model and—even more pronounced—in focal NMO (Fig. 2g, h). This may suggest a role of ADCC in NMO lesion propagation [29, 31, 44]. Recently, using a similar experimental approach, recombinant human anti-AQP4 antibodies co-injected with an NK cell line into the mouse brain produced large astrocyte-depleted lesions without accompanying demyelination [31]. While NK cells are reported to be scarce in human NMO tissue [34], neutrophils, eosinophils, and macrophages in NMO lesions may express Fcγ receptors and thus contribute to astrocyte damage via ADCC [29, 44].

Apart from their ability to lyse astrocytes via complement activation and ADCC [29, 31], anti-AQP4 antibodies binding to target astrocytes may initiate alternative pathogenic mechanisms [6, 8]. Internalization of AQP4 and EAAT2 after incubation of astrocytes without complement has been reported [7, 18] and may lead to deficient clearance of glutamate and secondary excitotoxic damage to brain parenchymal cells [7, 18]. Furthermore, altered water homeostasis may lead to myelin vacuolization [8]. Consistent with these observations, AQP4 loss in early inflammatory human NMO lesions regularly exceeds the area of GFAP, i.e., astrocyte, loss [32]. The relevance of these processes to NMO pathophysiology, however, remains uncertain. Internalization of AQP4 and EAAT2 was not observed after direct CNS injection of anti-AQP4 antibody [30], and anti-AQP4 autoantibodies did not inhibit water flux in reconstituted AQP4 proteoliposomes [33]. In both our models, immunohistochemical stainings for the astrocyte proteins GFAP, AQP4, EAAT2 and S100β showed nearly

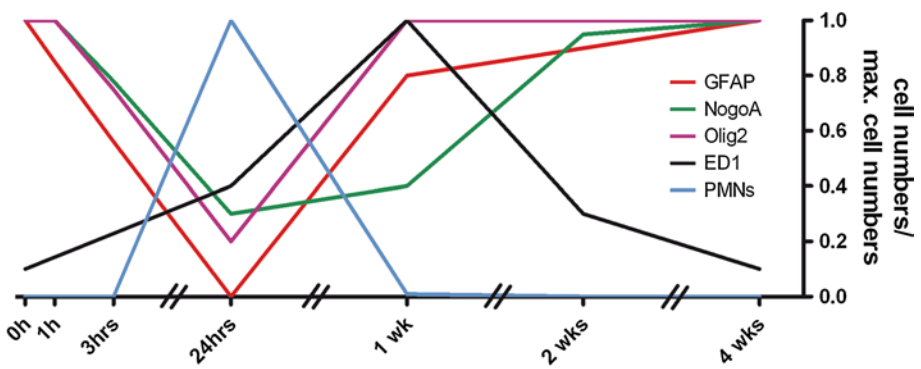

Fig. 9 Time course of parenchymal cell loss, inflammatory cell infiltration, and lesion repair in focal NMO. Cell numbers on the *y*-axis were normalized to maximum cell numbers

identical staining patterns in lesions, indicating that a selective downregulation of AQP4 or EAAT2 did not substantially contribute to lesion pathogenesis. A possible explanation could be the single administration of antibody leading to relatively even antibody distribution and only comparatively low antibody concentrations in the tissue.

Clinically and also pathologically, NMO is a demyelinating disease. The study of early human NMO lesions indicates a characteristic sequence of loss of myelin proteins, namely of MAG and CNP before MBP and PLP [4, 23]. Furthermore, dying oligodendrocytes were found in and at the edges of NMO lesions [4, 26]. These features are consistent with secondary demyelination induced by damage to oligodendrocytes. In both of our models that are dependent on complement-mediated astrocyte lysis, we show that oligodendrocyte death occurred within a few hours after astrocytic demise, even before substantial infiltration by granulocytes or macrophages/activated microglia was observed. Thus, mediators of oligodendrocyte injury independent of those released by granulocytes and activated microglia/macrophages are likely important [35]. The very rapid oligodendroglial death further argues against a lack of astroglial trophic factors playing a role in oligodendroglial demise. More likely, factors released by dying astrocytes, the loss of astrocytic buffering of toxic extracellular components (e.g., glutamate), alterations in the tissue microenvironment induced by astrocyte loss, or activated complement components may contribute to oligodendroglial death. Interestingly, mature NogoA-positive oligodendrocytes and Olig2-positive oligodendroglial precursor cells appeared equally susceptible to injury in our lesion models.

Marignier et al. showed that incubation of astrocytes with anti-AQP4 antibodies without complement was sufficient to induce a modest amount of astrocyte dysfunction associated with the accumulation of glutamate in the culture medium. Oligodendroglial cell death could be rescued in part by a glutamate antagonist [18]. In an optic nerve explant model, apoptotic oligodendrocytes were induced by supernatants of astrocytes treated with anti-AQP4 antibodies without complement or serum. Thus, astrocyte dysfunction could produce scattered oligodendroglial cell death, though not overt demyelination. As noted previously, in NMO-like lesions generated using anti-AQP4 antibodies and NK cells, no demyelination was observed after 4 days, indicating that oligodendroglial cell death is less pronounced or may be delayed in the absence of CDC [31]. Interestingly, astrocyte dysfunction after lipopolysaccharide injection also leads to oligodendroglial cell death, indicating the importance of astrocyte functionality for oligodendroglial survival [36].

Only scant evidence of oligodendroglial regeneration has thus far been reported in chronic human NMO lesions. However, astrocytic repopulation of NMO lesions is observed early after lesion formation and is morphologically characterized by bipolar, elongated astrocytes that are not seen in the usual post-inflammatory gliotic reaction, e.g., in MS lesions [4, 26]. The focal NMO model facilitates an assessment of the time course of lesion repair because the lesion site can still be identified after several weeks due to the injection of a marker dye. Thus, we found that astrocytic repair is already substantial 1 week after lesion induction. Similarly, Olig2-positive oligodendrocyte precursor cells were abundant in the lesion at this time point. However, mature NogoA-positive oligodendrocytes were still scarce and consequently, no signs of remyelination could be detected in the lesion center. This is in line with experimental data showing that astrocytes produce trophic factors necessary for oligodendroglial cells, and that no efficient oligodendroglial remyelination occurs in the absence of astrocytes [2]. Of note, repair may be facilitated in our focal model by the fact that—in contrast to the human disease—antibody is injected only once, and no blood-borne adaptive inflammatory reaction is present. An evaluation of the time course of lesion repair in the EAE/NMO model may assist in addressing these issues.

In conclusion, we report here that focal and systemic injection of human NMO rAb against AQP4 can reproduce important features of human NMO lesion pathology. Astrocytic death largely depends on complement activation, but also on ADCC, and oligodendroglial cell death occurs rapidly after astrocytic demise and precedes the infiltration of immune cells. Of note, astrocytic lesion repair is substantial within 1 week after lesion induction, and followed by oligodendroglial migration and differentiation. A more detailed understanding of lesion pathogenesis in NMO will help us to identify relevant targets for astrocyte, oligodendroglia, and myelin protection and repair.

Acknowledgments We acknowledge the excellent technical support by Brigitte Maruschak, Jasmin Reichl, Katja Schulz, Angela Dettmar, Heidi Brodmerkel, Olga Kowatsch and Uta Scheidt and thank Christine Crozier and Cynthia Bunker for their help with language editing. C.S. and W.B. were supported by the DFG (TR-SFB43 "The brain as a target of inflammatory processes"). J.L.B. was supported by grants from the Guthy-Jackson Foundation and the National Institutes of Health (EY022936). We are indebted to our patients and their relatives.

Conflict of interest The authors declare that they have no conflict of interest.

References

1. Bennett JL, Lam C, Kalluri SR, Saikali P, Bautista K, Dupree C, Glogowska M, Case D, Antel JP, Owens GP, Gilden D, Nessler S, Stadelmann C, Hemmer B (2009) Intrathecal pathogenic anti-aquaporin-4 antibodies in early neuromyelitis optica. Ann Neurol 66(5):617–629. doi:10.1002/ana.21802

2. Blakemore WF, Gilson JM, Crang AJ (2003) The presence of astrocytes in areas of demyelination influences remyelination following transplantation of oligodendrocyte progenitors. Exp Neurol 184(2):955–963. doi:10.1016/S0014-4886(03)00347-9
3. Bradl M, Misu T, Takahashi T, Watanabe M, Mader S, Reindl M, Adzemovic M, Bauer J, Berger T, Fujihara K, Itoyama Y, Lassmann H (2009) Neuromyelitis optica: pathogenicity of patient immunoglobulin in vivo. Ann Neurol 66(5):630–643. doi:10.1002/ana.21837
4. Bruck W, Popescu B, Lucchinetti CF, Markovic-Plese S, Gold R, Thal DR, Metz I (2012) Neuromyelitis optica lesions may inform multiple sclerosis heterogeneity debate. Ann Neurol 72(3):385–394. doi:10.1002/ana.23621
5. Furman CS, Gorelick-Feldman DA, Davidson KG, Yasumura T, Neely JD, Agre P, Rash JE (2003) Aquaporin-4 square array assembly: opposing actions of M1 and M23 isoforms. Proc Natl Acad Sci USA 100(23):13609–13614. doi:10.1073/pnas.2235843100
6. Hinson SR, Pittock SJ, Lucchinetti CF, Roemer SF, Fryer JP, Kryzer TJ, Lennon VA (2007) Pathogenic potential of IgG binding to water channel extracellular domain in neuromyelitis optica. Neurology 69(24):2221–2231. doi:10.1212/01.WNL.0000289761.64862.ce
7. Hinson SR, Roemer SF, Lucchinetti CF, Fryer JP, Kryzer TJ, Chamberlain JL, Howe CL, Pittock SJ, Lennon VA (2008) Aquaporin-4-binding autoantibodies in patients with neuromyelitis optica impair glutamate transport by down-regulating EAAT2. J Exp Med 205(11):2473–2481. doi:10.1084/jem.20081241
8. Hinson SR, Romero MF, Popescu BF, Lucchinetti CF, Fryer JP, Wolburg H, Fallier-Becker P, Noell S, Lennon VA (2012) Molecular outcomes of neuromyelitis optica (NMO)-IgG binding to aquaporin-4 in astrocytes. Proc Natl Acad Sci USA 109(4):1245–1250. doi:10.1073/pnas.1109980108
9. Jarius S, Aboul-Enein F, Waters P, Kuenz B, Hauser A, Berger T, Lang W, Reindl M, Vincent A, Kristoferitsch W (2008) Antibody to aquaporin-4 in the long-term course of neuromyelitis optica. Brain 131(Pt 11):3072–3080. doi:10.1093/brain/awn240
10. Kalluri SR, Rothhammer V, Staszewski O, Srivastava R, Petermann F, Prinz M, Hemmer B, Korn T (2011) Functional characterization of aquaporin-4 specific T cells: towards a model for neuromyelitis optica. PLoS ONE 6(1):e16083. doi:10.1371/journal.pone.0016083
11. Kinoshita M, Nakatsuji Y, Kimura T, Moriya M, Takata K, Okuno T, Kumanogoh A, Kajiyama K, Yoshikawa H, Sakoda S (2009) Neuromyelitis optica: passive transfer to rats by human immunoglobulin. Biochem Biophys Res Commun 386(4):623–627. doi:10.1016/j.bbrc.2009.06.085
12. Lennon VA, Kryzer TJ, Pittock SJ, Verkman AS, Hinson SR (2005) IgG marker of optic-spinal multiple sclerosis binds to the aquaporin-4 water channel. J Exp Med 202(4):473–477. doi:10.1084/jem.20050304
13. Lennon VA, Wingerchuk DM, Kryzer TJ, Pittock SJ, Lucchinetti CF, Fujihara K, Nakashima I, Weinshenker BG (2004) A serum autoantibody marker of neuromyelitis optica: distinction from multiple sclerosis. Lancet 364(9451):2106–2112. doi:10.1016/S0140-6736(04)17551-X
14. Linington C, Berger T, Perry L, Weerth S, Hinze-Selch D, Zhang Y, Lu HC, Lassmann H, Wekerle H (1993) T cells specific for the myelin oligodendrocyte glycoprotein mediate an unusual autoimmune inflammatory response in the central nervous system. Eur J Immunol 23(6):1364–1372. doi:10.1002/eji.1830230627
15. Linington C, Bradl M, Lassmann H, Brunner C, Vass K (1988) Augmentation of demyelination in rat acute allergic encephalomyelitis by circulating mouse monoclonal antibodies directed against a myelin/oligodendrocyte glycoprotein. Am J Pathol 130(3):443–454
16. Lucchinetti CF, Mandler RN, McGavern D, Bruck W, Gleich G, Ransohoff RM, Trebst C, Weinshenker B, Wingerchuk D, Parisi JE, Lassmann H (2002) A role for humoral mechanisms in the pathogenesis of Devic's neuromyelitis optica. Brain 125(Pt 7):1450–1461
17. Mandler RN, Davis LE, Jeffery DR, Kornfeld M (1993) Devic's neuromyelitis optica: a clinicopathological study of 8 patients. Ann Neurol 34(2):162–168. doi:10.1002/ana.410340211
18. Marignier R, Nicolle A, Watrin C, Touret M, Cavagna S, Varrin-Doyer M, Cavillon G, Rogemond V, Confavreux C, Honnorat J, Giraudon P (2010) Oligodendrocytes are damaged by neuromyelitis optica immunoglobulin G via astrocyte injury. Brain 133(9):2578–2591. doi:10.1093/brain/awq177
19. Matthieu JM, Waehneldt TV, Eschmann N (1986) Myelin-associated glycoprotein and myelin basic protein are present in central and peripheral nerve myelin throughout phylogeny. Neurochem Int 8(4):521–526 pii:0197-0186(86)90186-5
20. Merkler D, Boretius S, Stadelmann C, Ernsting T, Michaelis T, Frahm J, Bruck W (2005) Multicontrast MRI of remyelination in the central nervous system. NMR Biomed 18(6):395–403. doi:10.1002/nbm.972
21. Merkler D, Ernsting T, Kerschensteiner M, Bruck W, Stadelmann C (2006) A new focal EAE model of cortical demyelination: multiple sclerosis-like lesions with rapid resolution of inflammation and extensive remyelination. Brain 129(Pt 8):1972–1983. doi:10.1093/brain/awl135
22. Misu T, Fujihara K, Itoyama Y (2008) Neuromyelitis optica and anti-aquaporin 4 antibody—an overview. Brain Nerve 60(5):527–537
23. Misu T, Fujihara K, Kakita A, Konno H, Nakamura M, Watanabe S, Takahashi T, Nakashima I, Takahashi H, Itoyama Y (2007) Loss of aquaporin 4 in lesions of neuromyelitis optica: distinction from multiple sclerosis. Brain 130(Pt 5):1224–1234. doi:10.1093/brain/awm047
24. Nelson PA, Khodadoust M, Prodhomme T, Spencer C, Patarroyo JC, Varrin-Doyer M, Ho JD, Stroud RM, Zamvil SS (2010) Immunodominant T cell determinants of aquaporin-4, the autoantigen associated with neuromyelitis optica. PLoS ONE 5(11):e15050. doi:10.1371/journal.pone.0015050
25. Oertle T, van der Haar ME, Bandtlow CE, Robeva A, Burfeind P, Buss A, Huber AB, Simonen M, Schnell L, Brosamle C, Kaupmann K, Vallon R, Schwab ME (2003) Nogo-A inhibits neurite outgrowth and cell spreading with three discrete regions. J Neurosci 23(13):5393–5406. pii:23/13/5393
26. Parratt JD, Prineas JW (2010) Neuromyelitis optica: a demyelinating disease characterized by acute destruction and regeneration of perivascular astrocytes. Mult Scler 16(10):1156–1172. doi:10.1177/1352458510382324
27. Pohl M, Fischer MT, Mader S, Schanda K, Kitic M, Sharma R, Wimmer I, Misu T, Fujihara K, Reindl M, Lassmann H, Bradl M (2011) Pathogenic T cell responses against aquaporin 4. Acta Neuropathol 122(1):21–34. doi:10.1007/s00401-011-0824-0
28. Rash JE, Davidson KG, Yasumura T, Furman CS (2004) Freeze-fracture and immunogold analysis of aquaporin-4 (AQP4) square arrays, with models of AQP4 lattice assembly. Neuroscience 129(4):915–934. doi:10.1016/j.neuroscience.2004.06.076
29. Ratelade J, Asavapanumas N, Ritchie AM, Wemlinger S, Bennett JL, Verkman AS (2013) Involvement of antibody-dependent cell-mediated cytotoxicity in inflammatory demyelination in a mouse model of neuromyelitis optica. Acta Neuropathol 126(5):699–709. doi:10.1007/s00401-013-1172-z
30. Ratelade J, Bennett JL, Verkman AS (2011) Evidence against cellular internalization in vivo of NMO-IgG, aquaporin-4, and excitatory amino acid transporter 2 in neuromyelitis optica. J Biol Chem 286(52):45156–45164. doi:10.1074/jbc.M111.297275
31. Ratelade J, Zhang H, Saadoun S, Bennett JL, Papadopoulos MC, Verkman AS (2012) Neuromyelitis optica IgG and natural killer

cells produce NMO lesions in mice without myelin loss. Acta Neuropathol 123(6):861–872. doi:10.1007/s00401-012-0986-4
32. Roemer SF, Parisi JE, Lennon VA, Benarroch EE, Lassmann H, Bruck W, Mandler RN, Weinshenker BG, Pittock SJ, Wingerchuk DM, Lucchinetti CF (2007) Pattern-specific loss of aquaporin-4 immunoreactivity distinguishes neuromyelitis optica from multiple sclerosis. Brain 130(Pt 5):1194–1205. doi:10.1093/brain/awl371
33. Rossi A, Ratelade J, Papadopoulos MC, Bennett JL, Verkman AS (2012) Neuromyelitis optica IgG does not alter aquaporin-4 water permeability, plasma membrane M1/M23 isoform content, or supramolecular assembly. Glia 60(12):2027–2039. doi:10.1002/glia.22417
34. Saadoun S, Bridges LR, Verkman AS, Papadopoulos MC (2012) Paucity of natural killer and cytotoxic T cells in human neuromyelitis optica lesions. NeuroReport 23(18):1044–1047. doi:10.1097/WNR.0b013e32835ab480
35. Saadoun S, Waters P, Bell BA, Vincent A, Verkman AS, Papadopoulos MC (2010) Intra-cerebral injection of neuromyelitis optica immunoglobulin G and human complement produces neuromyelitis optica lesions in mice. Brain 133(Pt 2):349–361. doi:10.1093/brain/awp309
36. Sharma R, Fischer MT, Bauer J, Felts PA, Smith KJ, Misu T, Fujihara K, Bradl M, Lassmann H (2010) Inflammation induced by innate immunity in the central nervous system leads to primary astrocyte dysfunction followed by demyelination. Acta Neuropathol 120(2):223–236. doi:10.1007/s00401-010-0704-z
37. Takahashi T, Fujihara K, Nakashima I, Misu T, Miyazawa I, Nakamura M, Watanabe S, Shiga Y, Kanaoka C, Fujimori J, Sato S, Itoyama Y (2007) Anti-aquaporin-4 antibody is involved in the pathogenesis of NMO: a study on antibody titre. Brain 130(Pt 5):1235–1243. doi:10.1093/brain/awm062
38. Tradtrantip L, Zhang H, Saadoun S, Phuan PW, Lam C, Papadopoulos MC, Bennett JL, Verkman AS (2012) Anti-aquaporin-4 monoclonal antibody blocker therapy for neuromyelitis optica. Ann Neurol 71(3):314–322. doi:10.1002/ana.22657
39. Varrin-Doyer M, Spencer CM, Schulze-Topphoff U, Nelson PA, Stroud RM, Cree BA, Zamvil SS (2012) Aquaporin 4-specific T cells in neuromyelitis optica exhibit a Th17 bias and recognize *Clostridium* ABC transporter. Ann Neurol 72(1):53–64. doi:10.1002/ana.23651
40. Waters P, Jarius S, Littleton E, Leite MI, Jacob S, Gray B, Geraldes R, Vale T, Jacob A, Palace J, Maxwell S, Beeson D, Vincent A (2008) Aquaporin-4 antibodies in neuromyelitis optica and longitudinally extensive transverse myelitis. Arch Neurol 65(7):913–919. doi:10.1001/archneur.65.7.913
41. Waters PJ, McKeon A, Leite MI, Rajasekharan S, Lennon VA, Villalobos A, Palace J, Mandrekar JN, Vincent A, Bar-Or A, Pittock SJ (2012) Serologic diagnosis of NMO: a multicenter comparison of aquaporin-4-IgG assays. Neurology 78(9):665–671. doi:10.1212/WNL.0b013e318248dec1 (discussion 669)
42. Weissert R, Svenningsson A, Lobell A, de Graaf KL, Andersson R, Olsson T (1998) Molecular and genetic requirements for preferential recruitment of TCRBV8S2+ T cells in Lewis rat experimental autoimmune encephalomyelitis. J Immunol 160(2):681–690
43. Wolburg H, Wolburg-Buchholz K, Fallier-Becker P, Noell S, Mack AF (2011) Structure and functions of aquaporin-4-based orthogonal arrays of particles. Int Rev Cell Mol Biol 287:1–41. doi:10.1016/B978-0-12-386043-9.00001-3
44. Zhang H, Verkman AS (2013) Eosinophil pathogenicity mechanisms and therapeutics in neuromyelitis optica. J Clin Invest 123(5):2306–2316. doi:10.1172/JCI67554
45. Zhou D, Srivastava R, Nessler S, Grummel V, Sommer N, Bruck W, Hartung HP, Stadelmann C, Hemmer B (2006) Identification of a pathogenic antibody response to native myelin oligodendrocyte glycoprotein in multiple sclerosis. Proc Natl Acad Sci USA 103(50):19057–19062. doi:10.1073/pnas.0607242103